

Polar catastrophe and electronic reconstructions at the $\text{LaAlO}_3/\text{SrTiO}_3$ interface: evidence from optical second harmonic generation

A. Savoia,¹ D. Paparo,¹ P. Perna,¹ Z. Ristic,¹ M. Salluzzo,¹ F. Miletto Granozio,¹
U. Scotti di Uccio,¹ C. Richter,² S. Thiel,² J. Mannhart,² and L. Marrucci^{1,*}

¹*CNR-INFM Coherentia and Dipartimento di Scienze Fisiche, Università di Napoli “Federico II”,
Compl. Univ. di Monte S. Angelo, v. Cintia, 80126 Napoli, Italy*

²*Center for Electronic Correlations and Magnetism,
University of Augsburg, D-86135 Augsburg, Germany*

(Dated: November 26, 2024)

The so-called “polar catastrophe”, a sudden electronic reconstruction taking place to compensate for the interfacial ionic polar discontinuity, is currently considered as a likely factor to explain the surprising conductivity of the interface between the insulators LaAlO_3 and SrTiO_3 . We applied optical second harmonic generation, a technique that *a priori* can detect both mobile and localized interfacial electrons, to investigating the electronic polar reconstructions taking place at the interface. As the LaAlO_3 film thickness is increased, we identify two abrupt electronic rearrangements: the first takes place at a thickness of 3 unit cells, in the insulating state; the second occurs at a thickness of 4-6 unit cells, i.e., just above the threshold for which the samples become conducting. Two possible physical scenarios behind these observations are proposed. The first is based on an electronic transfer into localized electronic states at the interface that acts as a precursor of the conductivity onset. In the second scenario, the signal variations are attributed to the strong ionic relaxations taking place in the LaAlO_3 layer.

PACS numbers: 73.20.-r, 73.40.-c, 77.22.Ej, 42.65.Ky

I. INTRODUCTION

The observation that the interface between the two band insulators LaAlO_3 (LAO) and SrTiO_3 (STO) can be highly conducting¹ has spurred a flourishing of research activities, motivated both by the fundamental questions posed by this unexpected phenomenon and by the associated technological prospects (see, e.g., Refs. 2,3,4,5,6,7,8,9,10,11,12,13,14, or Refs. 15,16,17 for recent reviews). Since its initial discovery, several important features of this puzzling phenomenon have been well established. LAO-STO heterostructures consisting of a LAO film grown on the (001) surface of a STO substrate are only conducting if the interface shows a $(\text{LaO})^+ / (\text{TiO}_2)^0$ stacking, while they are insulating for $(\text{AlO}_2)^- / (\text{SrO})^0$ interfaces.¹ For well oxidized systems, the former interfaces are conducting only when the thickness of the LAO layer is at least 4 unit cells (u.c.), otherwise they are insulating.^{3,5} Moreover, the charge carriers are found to be localized in a interfacial layer that is only few nanometers thick^{3,5,11} and, below $\simeq 200$ mK, they give rise to two-dimensional superconductivity.⁷

A leading interpretation for this interfacial conductivity is based on the “polar catastrophe” mechanism (see, e.g., Ref. 2). The polar stacking of the charged LAO atomic planes on the neutral STO planes gives rise to an electrostatic potential difference across the LAO film that increases proportionally to its thickness and hence, for sufficiently thick LAO films, must be relaxed by an interfacial reconstruction. The latter could be ionic, involving lattice distortions and/or some degree of cationic mixing,^{2,4,8,18,19,20} but it has been proposed that an *electronic reconstruction* may instead be

the dominating effect, involving a transfer of electrons from LAO to STO, likely into the STO Ti $3d$ conduction band close to the interface, thus giving rise to the interfacial conduction.^{1,2,3,9,21,22,23} Although this model seems to provide an appealing explanation for many important features of the observed phenomena, there are issues left unresolved, and a general consensus on the correct physical interpretation has not been reached yet.¹⁵ One example of an unresolved issue is the difference between the electronic carrier density measured in well oxidized samples ($2 - 4 \times 10^{13} \text{ cm}^{-2}$)^{3,5} and that predicted by the polar catastrophe model ($3 \times 10^{14} \text{ cm}^{-2}$). A possible explanation for this “missing charge” problem is that part of the electrons injected into the interface are localized and therefore do not contribute to the conduction.²¹

To resolve this problem, and more generally to move forward in our understanding, it is desirable to directly probe the rearrangements of all interfacial electrons, rather than of the mobile carriers only. *Second harmonic generation* (SHG), a nonlinear optical technique based on the detection of doubled-frequency photons in the light reflected (or transmitted) from the interface, provides just this capability.²⁴ When the illuminated materials are centrosymmetric, second-harmonic (SH) photons are generated with high efficiency only in the thin interfacial regions in which the inversion symmetry of the electronic orbitals is broken. SHG has already been successfully applied to studying interfaces between other perovskite oxides^{25,26} and, concurrently to the present work, to LAO/STO superlattices.²⁷ Using SHG, variations in the degree of interfacial polarity associated with electronic reconstructions are expected to be detectable with high sensitivity. The SHG signal can be regarded

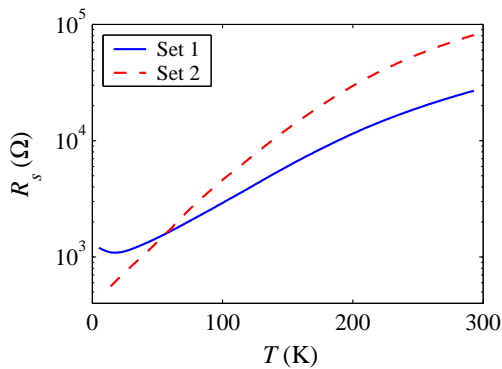


FIG. 1: (color online). Sheet resistance versus temperature for two LAO/STO conducting samples having LAO thickness $d = 4$ u.c., one from set 1 (solid line, blue) and the other from set 2 (dashed line, red). In both a metallic behavior is evident, with a small resistance increase for the sample of set 1 at low temperatures.

as a “weighted average” of the degree of polar asymmetry felt by all electrons present in the system, with a weight given approximately by the electron polarizability at optical frequencies. In the present work, we have used SHG to analyze the LAO/STO system in a set of samples in which the thickness d of the LAO layers was varied from an undercritical thickness with insulating interfaces, through the critical thickness, up to thick LAO layers which generate well conducting samples.

II. EXPERIMENT

LAO films were grown by pulsed laser deposition on STO(001) substrates with TiO_2 plane termination, while controlling the LAO thickness on a unit cell scale using high-energy electron diffraction (RHEED) oscillations. A first set of samples (set 1, manufactured in Naples) was grown at ≈ 800 °C in an oxygen atmosphere of 1×10^{-4} mbar, and then cooled at the same pressure to room temperature. A second set of samples (set 2, manufactured in Augsburg) was prepared in 8×10^{-5} mbar of O_2 at 770 °C and cooled in 400 mbar of O_2 . In both sets, interfacial conduction appears only for a LAO thickness $d \geq 4$ u.c., in agreement with previous results.³ Two examples of the typical resistivity temperature-dependence of conducting samples are shown in Fig. 1. An additional $d = 3$ u.c. sample of set 2 was fabricated with a back-gate for field-effect switching.³ Hall measurements yielded interfacial carrier densities of $\sim 10^{14} \text{ cm}^{-2}$ in conducting samples of set 1 and of $\sim 10^{13} \text{ cm}^{-2}$ in those of set 2 (at 300 K). All SHG measurements were performed at room temperature in air and in dark (the samples were also kept in dark for 24 hours before the measurements), after cleaning the sample surfaces with isopropyl alcohol.

The schematic of our SHG experiment is shown in Fig. 2. A Nd:YAG mode-locked laser delivered 20 ps long

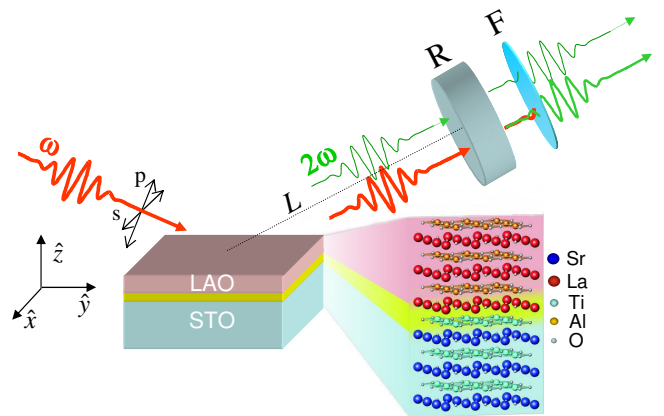


FIG. 2: (color online). Schematic of the homodyne SHG experiment. The sample is irradiated with laser pulses at frequency ω (drawn in red). The SH light (2ω , in green) generated in reflection by the upper surface of the sample (including the interface) is made to interfere with the SH generated by a reference quartz crystal (R) illuminated by the reflected beam at the fundamental frequency (for clarity, in the figure the two beams are shown as being spatially separated; in reality, they are almost perfectly collinear and superimposed). The latter is moved along the beam path (with displacement L), so as to modulate the phase difference of the two SH terms by exploiting air dispersion. A filter (F) stops the reflected light of frequency ω before detection. The incidence angle is 64° . The input/output polarizations s and p used in our experiments are also shown, with s denoting an optical electric field parallel to the sample surface xy , and p a field lying in the incidence plane yz .

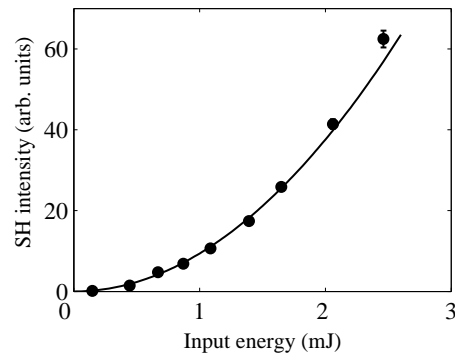


FIG. 3: Example of the SHG signal intensity (dots) detected for increasing input pulse energy (sample of set 1 with $d = 6$ u.c.); the line is a quadratic best-fit.

pulses at a repetition rate of 10 Hz, which were focused on the sample with an energy of ≈ 2 mJ in a spot-area of $\approx 1 \text{ mm}^2$. The input photon energy of 1.17 eV (1064 nm) is well below the gap energy of both LAO (5.6 eV) and STO (3.3 eV), so that all possible photoinduced effects are minimized. The SHG intensity signal from all samples was found to be stable in time and to vary quadratically with the input laser energy (Fig. 3), confirming that the interface properties were not noticeably altered by the irradiation. The laser irradiation was also found not to

induce any significant photoconductivity. For our measurements, the SHG beam generated in reflection from the upper surface of the samples was selected. Because the LAO film thickness is very small as compared to the optical wavelength, this SHG signal may include contributions of the LAO upper surface and of the LAO/STO interface, without significant propagation-induced phase-shifts between them. For a given optical geometry, the SHG signal of the entire interfacial region is determined by its integrated effective nonlinear susceptibility

$$\chi_{\text{eff}}^{(2)} = \int e_i^{\text{out}} L_{ii}^{\text{out}}(z) \chi_{ijh}^{(2)}(z) L_{jj}^{\text{in}}(z) L_{hh}^{\text{in}}(z) e_j^{\text{in}} e_h^{\text{in}} dz, \quad (1)$$

where $\chi_{ijh}^{(2)}(z)$ are the local second-order nonlinear susceptibility tensor elements, $L_{ii}^{\text{in/out}}(z)$ the input/output Fresnel field factors accounting for the optical propagation, $e_i^{\text{in/out}}$ are the unit vectors of the input/output polarization directions (sum over repeated indices is understood), and z a coordinate along the interface normal.²⁴ Standard SHG measurements give a signal that is proportional to the squared-modulus $|\chi_{\text{eff}}^{(2)}|^2$. This quantity, or its square-root $|\chi_{\text{eff}}^{(2)}|$, provides an estimate of the “degree of polarity” of the interface electrons. More information on the electronic rearrangements, for example the *direction of the polar asymmetry* (which determines the sign of the $\chi_{\text{eff}}^{(2)}$), is derived from the full $\chi_{\text{eff}}^{(2)}$, which in general is a complex quantity. To measure the $\chi_{\text{eff}}^{(2)}$, we adopted a homodyne SHG (HSHG) detection geometry²⁸ as described in Fig. 2. Examples of the resulting interference fringes are shown in Fig. 4. With suitable fitting,²⁸ such patterns allowed us to obtain for each sample both modulus and phase of the complex $\chi_{\text{eff}}^{(2)}$ (up to a constant phase, which is the same for all measurements sharing the same experimental geometry). These measurements were performed for the four input/output polarization combinations *ss*, *ps*, *sp*, *pp* (see Fig. 2), each corresponding to a different $\chi_{\text{eff}}^{(2)}$, which in the following will be respectively denoted as $\chi_{ss}^{(2)}$, $\chi_{ps}^{(2)}$, $\chi_{sp}^{(2)}$, $\chi_{pp}^{(2)}$. All SHG measurements with *s* output yielded negligible signals, i.e. we find $\chi_{ss}^{(2)} \simeq 0$ and $\chi_{ps}^{(2)} \simeq 0$, as expected for the C_{4v} symmetry of our interfaces. We note that both the vanishing of the *s*-polarized SHG and the reproducibility of our HSHG phase measurements confirm that our signal is coming from the interface and not resulting from hyper-Rayleigh scattering from the STO substrate.

III. RESULTS AND DISCUSSION

Figures 5a-b show the amplitude (modulus) of the *sp* and *pp* effective nonlinear susceptibilities measured as a function of the LAO film thickness d . We note that STO substrates ($d = 0$) already generate a significant signal. In contrast, we measured a negligible SHG from the (001) surface of a LAO single crystal. In LAO/STO

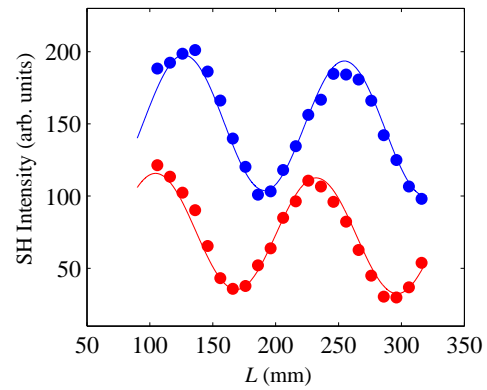


FIG. 4: (color online). Two examples of SH interference fringes observed in our HSHG experiments (*sp* polarizations) for samples of set 1 having LAO thickness $d = 3$ u.c. (lower curve, red dots) and $d = 4$ u.c. (upper curve, blue dots).

heterostructures, the SH amplitude $|\chi_{sp}^{(2)}|$ is seen to be approximately constant for $0 \leq d \leq 2$ u.c. with only a slight decrease observed for samples having 1 or 2 monolayers of LAO with respect to bare STO substrates (Fig. 5a). When the LAO thickness reaches $d = 3$ u.c., however, an abrupt and substantial increase of the SHG intensity takes place. The SHG signal obtained for different 3 u.c. samples also exhibits a strong scatter, that is not seen for other thicknesses. Both observations indicate that $d = 3$ u.c. is the threshold value for a discontinuous structural transition. For larger d , the SHG amplitude increases further to saturate or to decrease again for $d \gtrsim 10$ u.c. (with some scatter from sample to sample). This step-like behavior is clearly evident for the samples of set 1. For samples of set 2 the signal is smaller and the transition seems more gradual. This fact implies that more electrons are involved in the interfacial process for samples of set 1 as compared to those of set 2, in accordance with the difference of the measured carrier densities. In the *pp* geometry (Fig. 5b), samples of set 1 behave quite similarly to the *sp* case, while samples of set 2 show a more complex behavior, with a decrease of SH intensity at $d = 2$ u.c. and an increase at $d = 6$ u.c. In this case, however, a step-like behavior of the imaginary component of $\chi_{pp}^{(2)}$ is still seen (inset of Fig. 5b).

The measured behavior of the SHG is reminiscent of the abrupt conductance change that is found in the samples as a function of d (Fig. 5c). However, the conduction step occurs for $d \geq 4$ u.c., while the SHG step has been found to take place for $d \geq 3$ u.c. This implies that the SHG signal is not detecting directly the mobile electrons, but it is instead *revealing a related phenomenon that acts as a precursor for the onset of conductivity*. This important conclusion is further confirmed by the observation that the HSHG signal is not sensitive to the switch in conductivity that can be induced in a $d = 3$ u.c. sample by an applied back-gate voltage (Fig. 5d). On the other hand, SHG is not expected to be specifically sensitive

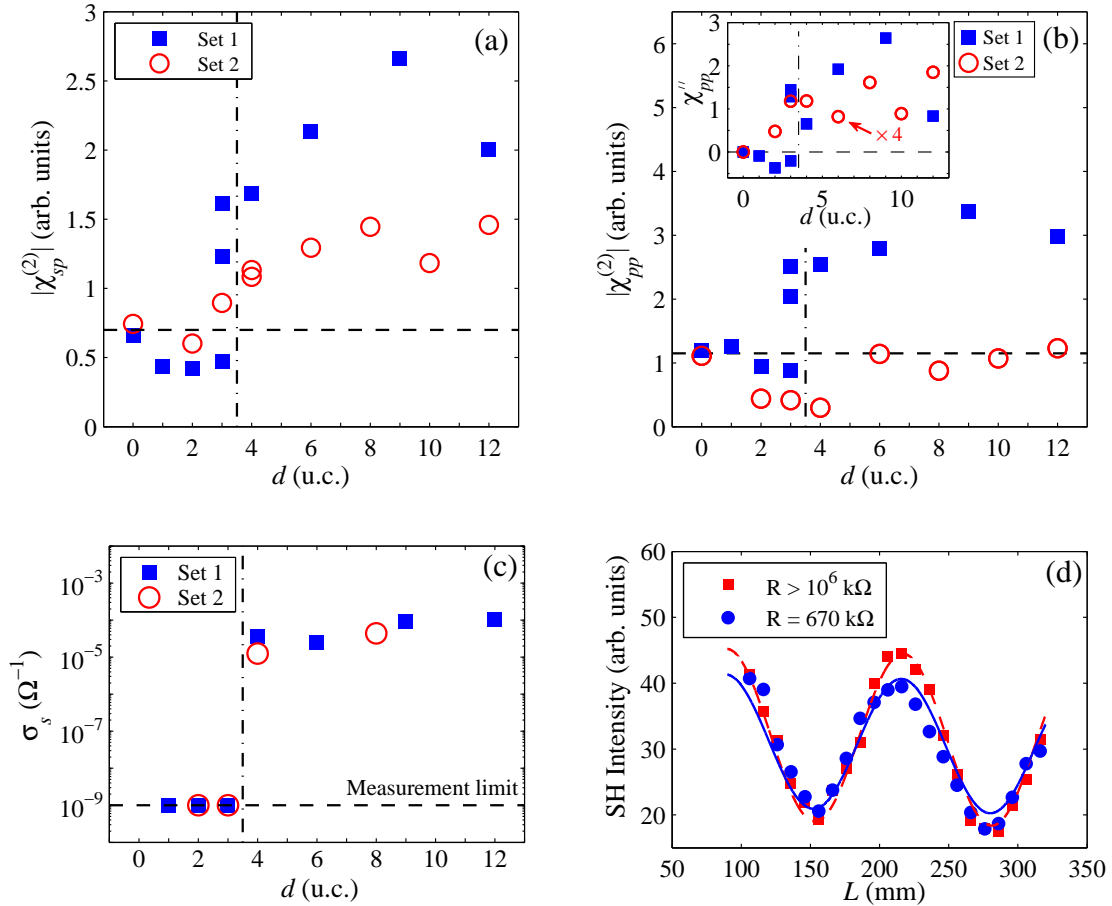


FIG. 5: (color online). Panels (a)-(b): Amplitude of the SHG effective nonlinear susceptibilities $\chi_{sp}^{(2)}$ (a) and $\chi_{pp}^{(2)}$ (b) measured as a function of LAO thickness d for samples of set 1 (blue squares) and set 2 (red circles). Different data points with the same d refer to different samples. The dashed horizontal line gives the average SHG amplitude of the STO substrates ($d = 0$). The dot-dashed vertical line corresponds to the measured threshold thickness (i.e., between 3 and 4 u.c.) for the onset of conductivity. Inset of panel (b): imaginary component of $\chi_{pp}^{(2)}$ (data of set 2 are rescaled by a factor 4 for clarity). Panel (c): Sheet conductivity measured for most of our samples; note that all four samples with $d = 3$ u.c. were found to be insulating, in the absence of external fields. Panel (d): HSHG sp signal for a $d = 3$ u.c. sample of set 2 in its insulating (red squares) and conductive (blue circles) state, respectively obtained by applying -100 V and $+100$ V to a back-gate.³ All data were taken at room temperature.

to the conduction itself. An increase of the SHG amplitude may reflect, in general, either an increase of polarizing electric fields experienced by the interfacial electrons (possibly also reflecting lattice distortions) or a transfer of electrons from less polarizable and/or less polar orbitals to more polarizable and/or more polar ones.

The full complex nonlinear susceptibility $\chi_{\text{eff}}^{(2)}$ provides further useful information on the electronic behavior of the interfaces. It is convenient to present these data in a complex plane: in this representation, the extent of the electronic rearrangements that result from each addition of a monolayer of LAO is directly related to the distance between consecutive data points in the plane. As Fig. 6 shows, also the data of complex susceptibility exhibit large variations at $d = 3$ u.c. (green solid-line arrows),

but small ones for thinner LAO layers. For larger d , however, another abrupt and large variation of the HSHG signal is found (red dashed-line arrows in Fig. 6). Because this is mainly a phase variation, it is not well visible in the amplitude plots discussed above. Such a phase shift in the nonlinear susceptibility can only result from an electronic transfer, as optical phase retardations are determined by the optical resonances of the electronic polarizability. Samples in set 1 (Fig. 6a,c) exhibit this second transition between $d = 3$ u.c. and $d = 4$ u.c. (see also Fig. 4), i.e., in coincidence with the onset of conduction. The samples of set 2 (Fig. 6b,d) also show this second transition. Yet, they behave a bit differently: the change of $\chi_{\text{eff}}^{(2)}$ at $d = 4$ u.c. is small, and the second transition is seen only when passing from 4 u.c. to 6 u.c. Also this difference in the behavior of the two sample sets

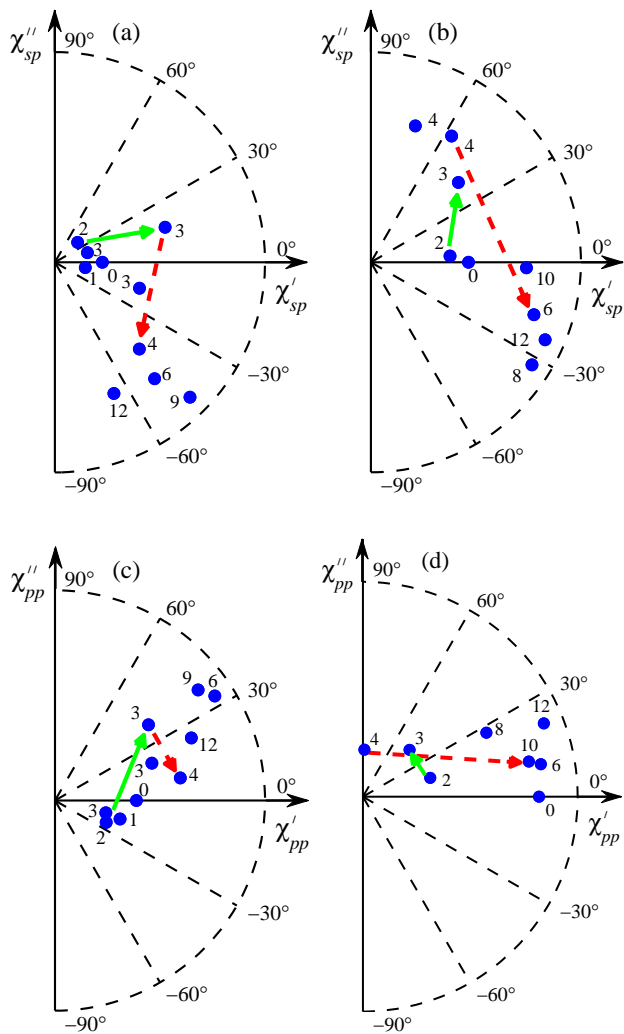


FIG. 6: (color online). Complex effective SHG nonlinear susceptibility $\chi_{sp}^{(2)} = \chi'_{sp} + i\chi''_{sp}$ (panels a and b) and $\chi_{pp}^{(2)} = \chi'_{pp} + i\chi''_{pp}$ (panels c and d) of the LAO/STO heterostructure for samples of set 1 (a and c) and set 2 (b and d) having different LAO thicknesses d . The polar angle of each point corresponds to the argument (or phase) of the complex susceptibility, as measured by HSHG (defined to zero for $d = 0$). The numbers typed next to the data points give the thicknesses of the LAO films in u.c. The two arrows in each panel (solid-line green and dashed-line red) indicate the two abrupt electronic transitions discussed in the text.

is likely related with the larger overall density of electrons involved in the interfacial process for set 1, leading, at this second transition, to a “faster” variation with d .

IV. POSSIBLE INTERPRETATIONS

Two main alternative scenarios are seen as candidates of the electronic effects underlying the two transitions observed with HSHG.

Scenario 1 is based on the assumption that the SHG

signal is dominated by the electronic states residing in the STO because its electric and optical polarizabilities far exceed those of LAO. This assumption is also suggested by the observation of a negligible SHG from the LAO single crystal. In this scenario, at a LAO thickness of 3 u.c. the “polar catastrophe” begins and electrons start to be injected from LAO into STO interface states. Because interfaces with $d = 3$ u.c. are insulating, these electrons must be trapped in localized surface states. Although not mobile, these electrons provide the main contribution to the first SHG transition. The possible presence of localized electrons at the LAO/STO interface has been addressed in several studies, in connection with strong-correlation effects, lattice deformations, self-trapped polarons, etc. (see, e.g., Refs. 4,18,29,30,31), and may be related to the magnetic effects seen in suitable conditions at low temperatures.⁶ A particularly intriguing possibility is that the trapping mechanism is a form of disorder-driven Anderson localization taking place in the quasi-two-dimensional electron gas.²¹ Recent evidence of extreme sensitivity of carrier concentrations to relatively small interface delta-doping favors this hypothesis.³² Disorder at $d = 3$ u.c. may be strongly enhanced by the intrinsic electronic bistability of the system,^{10,14} which might be also reflected in the large sample-to-sample variability observed in our SHG signal. It is also possible that such bistability gives rise to a phase-separation at the interface, with non-percolating conducting regions surrounded by insulating ones. On further increasing the LAO film thickness, more electrons are injected and give rise to conduction. The onset of conduction may be related with a reduced disorder (as bistability is not observed for $d \geq 4$ u.c.) or it may arise because electrons start to occupy higher-energy interfacial orbitals, e.g., different Ti $3d-t_{2g}$ subbands,^{21,33,34} including extended states. Within this scenario, we would ascribe, in particular, the second SHG transition seen in the polar plots of Fig. 6 to the filling of higher-energy interfacial subbands. Our SHG findings would then be consistent with the localized-electrons explanation of the missing charge problem.²¹

Scenario 2 assumes that the contribution to SHG of the LAO orbitals is not negligible and that at $d = 3$ u.c. the polarity of the LAO layer suddenly increases. The electronic polarity of thinner LAO films may be depressed, e.g., by interfacial roughness, cationic mixing,^{2,8} or lattice distortions.^{4,19,20} These effects could be particularly large in the two outer monolayers of the LAO film that are adjacent to the STO and to the air, possibly explaining the 3 u.c. threshold. *Ab initio* calculations of the ionic relaxations taking place in the LAO film support in part this concept, as the ionic relaxation is indeed predicted to be weak in the outermost atomic planes of LAO.²⁰ In this scenario, only the second transition seen by SHG is ascribed to the LAO→STO electronic injection. We believe this second scenario to be less likely than the first one, but it cannot be excluded at present.

V. CONCLUSIONS

In summary, the interfacial reconstructions taking place in LAO/STO heterostructures as a function of the LAO thickness have been investigated by using optical second harmonic generation. Two distinct electronic transitions were found, which result from the reorganization of the electrons at the LAO/STO interface induced by the polar discontinuity. In the most plausible interpretation scenario, the second-harmonic signal provides evidence that, at the critical LAO thickness of 3 unit cells, electrons are already injected in the interface but become localized. This might be linked to the recently demonstrated electronic bistability of the interface at this critical thickness, which can give rise to disorder-driven Anderson localization or, possibly, a complete phase separation between conducting and insulating areas. For

higher LAO thickness the number of injected electrons increases and their distribution becomes more uniform, thus giving rise to the observed conduction. In addition, evidence for the existence of distinct interfacial electronic subbands is provided by the second transition in the optical signal seen for increasing LAO thickness.

Acknowledgments

We thank Daniele Marré, Ilaria Pallecchi, and Marta Codda for Hall measurements, Davide Maccariello for help in the sample growth, and Marco Siano and Romolo Savo for help in some SHG measurements. This work was supported by the EU (Nanoxide) and by the DFG (SFB484).

-
- * Electronic address: lorenzo.marrucci@na.infn.it
- ¹ A. Ohtomo and H. Y. Hwang, *Nature (London)* **427**, 423 (2004).
 - ² N. Nakagawa, H. Y. Hwang, and D. A. Muller, *Nature Mat.* **5**, 204 (2006).
 - ³ S. Thiel, G. Hammerl, A. Schmehl, C. W. Schneider, and J. Mannhart, *Science* **313**, 1942 (2006).
 - ⁴ V. Vonk, M. Huijben, K. J. I. Driessen, P. Tinnemans, A. Brinkman, S. Harkema, and H. Graafsma, *Phys. Rev. B* **75**, 235417 (2007).
 - ⁵ W. Siemons, G. Koster, H. Yamamoto, W. A. Harrison, G. Lucovsky, T. H. Geballe, D. H. A. Blank, and M. R. Beasley, *Phys. Rev. Lett.* **98**, 196802 (2007).
 - ⁶ A. Brinkman, M. Huijben, M. V. Zalk, J. Uijben, U. Zeitler, J. C. Maan, W. G. V. der Wiel, G. Rijnders, D. H. A. Blank, and H. Hilgenkamp, *Nature Mat.* **6**, 493 (2007).
 - ⁷ N. Reyren, S. Thiel, A. D. Caviglia, L. F. Kourkoutis, G. Hammerl, C. Richter, C. W. Schneider, T. Kopp, A.-S. Rüetschi, D. Jaccard, et al., *Science* **317**, 1196 (2007).
 - ⁸ P. R. Willmott, S. A. Pauli, R. Herger, C. M. Schlepütz, D. Martocchia, B. D. Patterson, B. Delley, R. Clarke, D. Kumah, C. Cionca, et al., *Phys. Rev. Lett.* **99**, 155502 (2007).
 - ⁹ Y. Hotta, T. Susaki, and H. Y. Hwang, *Phys. Rev. Lett.* **99**, 236805 (2007).
 - ¹⁰ C. Cen, S. Thiel, G. Hammerl, C. W. Schneider, K. E. Andersen, C. S. Hellberg, J. Mannhart, and J. Levy, *Nature Mat.* **7**, 298 (2008).
 - ¹¹ M. Basletić, J.-L. Maurice, C. Carrétéro, G. Herranz, O. Copie, M. Bibes, E. Jacquet, K. Bouzehouane, S. Fusil, and A. Barthélémy, *Nature Mat.* **7**, 621 (2008).
 - ¹² K. Yoshimatsu, R. Yasuhara, H. Kumigashira, and M. Oshima, *Phys. Rev. Lett.* **101**, 026802 (2008).
 - ¹³ A. D. Caviglia, S. Gariglio, N. Reyren, D. Jaccard, T. Schneider, M. Gabay, S. Thiel, G. Hammerl, J. Mannhart, and J.-M. Triscone, *Nature* **456**, 624 (2008).
 - ¹⁴ C. Cen, S. Thiel, J. Mannhart, and J. Levy, *Science* **323**, 1026 (2009).
 - ¹⁵ S. A. Pauli and P. R. Willmott, *J. Phys.: Condens. Matter.* **20**, 264012 (2008).
 - ¹⁶ J. Mannhart, D. H. A. Blank, H. Y. Hwang, A. J. Millis, and J.-M. Triscone, *MRS Bull.* **33**, 1027 (2008).
 - ¹⁷ M. Huijben, A. Brinkman, G. Koster, G. Rijnders, H. Hilgenkamp, and D. H. A. Blank, *Adv. Mater.* **21**, 1665 (2009).
 - ¹⁸ Z. Zhong and P. Kelly, *Europhys. Lett.* **84**, 27001 (2008).
 - ¹⁹ C. L. Jia, S. B. Mi, M. Faley, U. Poppe, J. Schubert, and K. Urban, *Phys. Rev. B* **79**, 081405 (2009).
 - ²⁰ R. Pentcheva and W. E. Pickett, *Phys. Rev. Lett.* **102**, 107602 (2009).
 - ²¹ Z. S. Popović, S. Satpathy, and R. M. Martin, *Phys. Rev. Lett.* **101**, 256801 (2008).
 - ²² H. Chen, A. M. Kolpak, and S. Ismail-Beigi, *Phys. Rev. B* **79**, 161402(R) (2009).
 - ²³ M. Sing, G. Berner, K. Goß, A. Müller, A. Ruff, A. Wetscherek, S. Thiel, J. Mannhart, S. A. Pauli, C. W. Schneider, et al., *Phys. Rev. Lett.* **102**, 176805 (2009).
 - ²⁴ Y. R. Shen, *Surface Science* **299/300**, 551 (1994).
 - ²⁵ H. Yamada, Y. Ogawa, Y. Ishii, H. Sato, M. Kawasaki, H. Akoh, and Y. Tokura, *Science* **305**, 646 (2004).
 - ²⁶ N. Ogawa, T. Satoh, Y. Ogimoto, and K. Miyano, *Phys. Rev. B* **78**, 212409 (2008).
 - ²⁷ N. Ogawa, K. Miyano, M. Hosoda, T. Higuchi, C. Bell, Y. Hikita, and H. Y. Hwang, arXiv:0902.0070v1 (2009).
 - ²⁸ J. I. Dadap, J. Shan, A. S. Weling, J. A. Misewich, and T. F. Heinz, *Appl. Phys. B* **68**, 333 (1999).
 - ²⁹ R. Pentcheva and W. E. Pickett, *Phys. Rev. B* **78**, 205106 (2008).
 - ³⁰ R. Pentcheva and W. E. Pickett, *Phys. Rev. B* **74**, 035112 (2006).
 - ³¹ A. Rubano, D. Paparo, F. Miletto, U. Scotti di Uccio, and L. Marrucci, *Phys. Rev. B* **76**, 125115 (2007).
 - ³² T. Fix, J. L. MacManus-Driscoli, and M. G. Blamire, *Appl. Phys. Lett.* **94**, 172101 (2009).
 - ³³ M. Salluzzo, J. C. Cezar, N. B. Brookes, V. Bisogni, G. M. D. Luca, C. Richter, S. Thiel, J. Mannhart, M. Huijben, A. Brinkman, et al., *Phys. Rev. Lett.* **102**, 166804 (2009).
 - ³⁴ O. Copie, V. Garcia, C. Bödefeld, C. Carrétéro, M. Bibes, G. Herranz, E. Jacquet, J.-L. Maurice, B. Vinter, S. Fusil, et al., *Phys. Rev. Lett.* **102**, 216804 (2009).